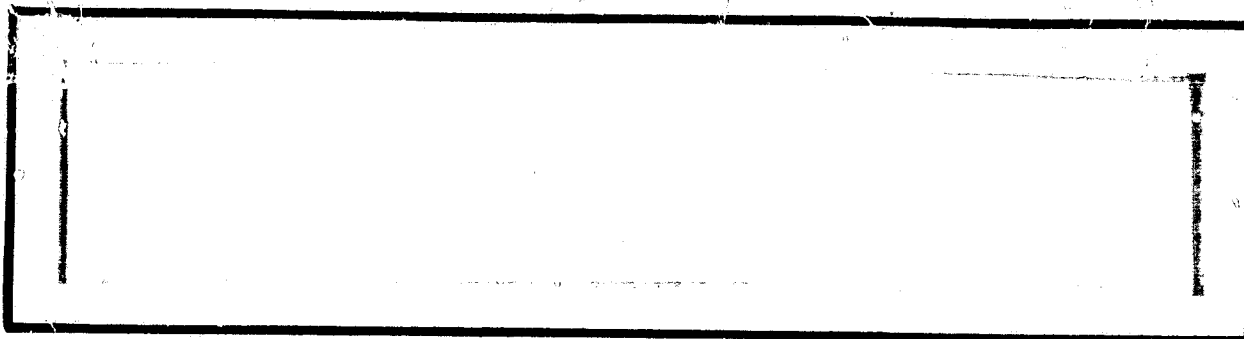


## N O T I C E

THIS DOCUMENT HAS BEEN REPRODUCED FROM  
MICROFICHE. ALTHOUGH IT IS RECOGNIZED THAT  
CERTAIN PORTIONS ARE ILLEGIBLE, IT IS BEING RELEASED  
IN THE INTEREST OF MAKING AVAILABLE AS MUCH  
INFORMATION AS POSSIBLE

NASA CR-

160557



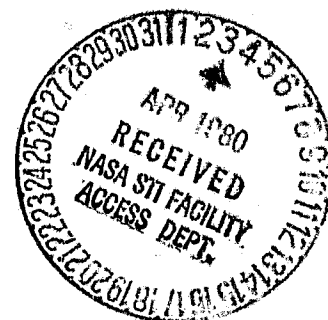
# Axiomatix

(NASA-CR-160557) Ku-BAND RADAR THRESHOLD  
ANALYSIS (Axiomatix, Los Angeles, Calif.)  
37 p HC A03/MP A01 CSCL 17I

N80-19322

Unclass

G3/32 47544



KU-BAND RADAR THRESHOLD ANALYSIS

Contract NAS 9-15795

(Technical Monitor: E. B. Walters)

Prepared for

NASA Lyndon B. Johnson Space Center  
Houston, Texas 77058

Prepared by

C. L. Weber  
A. Polydoros  
Axiomatix  
9841 Airport Blvd., Suite 912  
Los Angeles, California 90045

Axiomatix Report No. R8001-2  
January 11, 1979

# GLOSSARY OF SYMBOLS

$I$  = RF frequency index;  $I \in [1, I_{\max}]$

$L$  = Range gate index;  $\begin{cases} -1: & \text{early gate} \\ +1: & \text{late gate} \end{cases}$

$k$  = Time index for a specified pair  $(I, L)$ ;  $k \in [0, N-1]$

$m$  = Doppler filter index;  $m \in [0, N-1]$ ,  $N = 16$

$S_R(L, k)$ ,  $S_I(L, k)$  = Real and imaginary parts, respectively, of the signal component at the output of the  $L$ th range gate, at time  $k$ .

$N_R(L, k)$ ,  $N_I(L, k)$  = Real and imaginary parts, respectively, of the noise component at the output of the  $L$ th gate, at time  $k$ .

$\frac{PSI(L, k)}{S_R(L, k) + N_R(L, k)}$  = Real part of the total output of the  $L$ th gate at time  $k$ .

$\frac{PSQ(L, k)}{S_I(L, k) + N_I(L, k)}$  = Imaginary part of the total output of the  $L$ th gate at time  $k$ .

$F(L, m)$  = Output of the  $m$ th doppler filter following the  $L$ th gate.

$F_R(L, m)$ ,  $F_I(L, m)$  = Real and imaginary parts of  $F(L, m)$ , respectively.

$\sigma_s^2$  = Variance of the in-phase and quadrature phase Gaussian signal components.

$\sigma_n^2$  = Variance of the in-phase and quadrature phase Gaussian noise components.

$N$  = Order of the Discrete Fourier Transform (DFT) filter.

$|\cdot|$  = Norm of  $(\cdot)$

$\rho$  = Noise correlation coefficient.

$j = \sqrt{-1}$

## SUMMARY

In this report, the statistics of the CFAR threshold for the Ku-band radar are determined. Exact analytical results are developed for both the mean and standard deviations in the designated search mode. The mean value is compared to the results of a simulation reported in [1]. The analytical results are more optimistic than the simulation results, for which no explanation is offered.

The normalized standard deviation is shown to be very sensitive to signal-to-noise ratio and very insensitive to the noise correlation present in the range gates of the designated search mode. The substantial variation in the CFAR threshold is dominant at large values of SNR where the normalized standard deviation is greater than 0.3. Whether or not this significantly affects the resulting probability of detection is a matter which deserves additional attention.

On the optimistic side, the threshold setting and target return are correlated; this leads us to conjecture that this variation may not appreciably affect the probability of detection. On the pessimistic side, there is a substantial variation of the CFAR threshold setting away from that developed from the noise-only condition.

The constant false alarm rate (CFAR) thresholding scheme in the Shuttle Ku-band radar is analyzed for the "designated mode" of operation. In particular, both the mean and standard deviations are determined for the threshold level.

In search, there are two basic modes of operation: designated and undesignated. In the designated mode, range being designated, there are two overlapping range gates of width  $3\tau/2$ , where  $\tau$  is the transmitted pulse width. Four nonoverlapping range gates of width  $\tau$  are used in the undesignated mode.

Sixteen pulses are transmitted at each of the five RF frequencies. When range designation is available, the pulse width and pulse repetition frequency are functions of the designated range.

## 2.0 DESIGNATED MODE THRESHOLD

The basic signal processing of the Shuttle Ku-band radar for the designated mode in search is shown in Figure 1. Only those signal processings pertinent to the CFAR threshold formulation are shown. For a more detailed description of the signal processing for the Ku-band radar, see [2].

The output of the IF filter is downconverted to a complex base-band waveform

$$I + jQ = SI(I,J,k) + jSQ(I,J,k) \quad (1)$$

Before A/D, the I and Q waveforms for the  $k$ th pulse are given by

$$I + jQ = A_I P(t - kT_p) \exp[j(\omega_d t + \theta_I)] + N_c(t) + jN_s(t) \quad (2)$$

where

$A_I$  = the random amplitude of the target return which has the Rayleigh probability density function with parameter  $\sigma_s^2$ , which represents signal power

$\theta_I$  = a random phase uniformly distributed over  $(0, 2\pi)$

$\omega_d$  = the doppler frequency, which is neglected in this analysis. The effect of doppler on the final results is not expected to be appreciable.

$P(t)$  = pulse shape of width  $\tau$  seconds

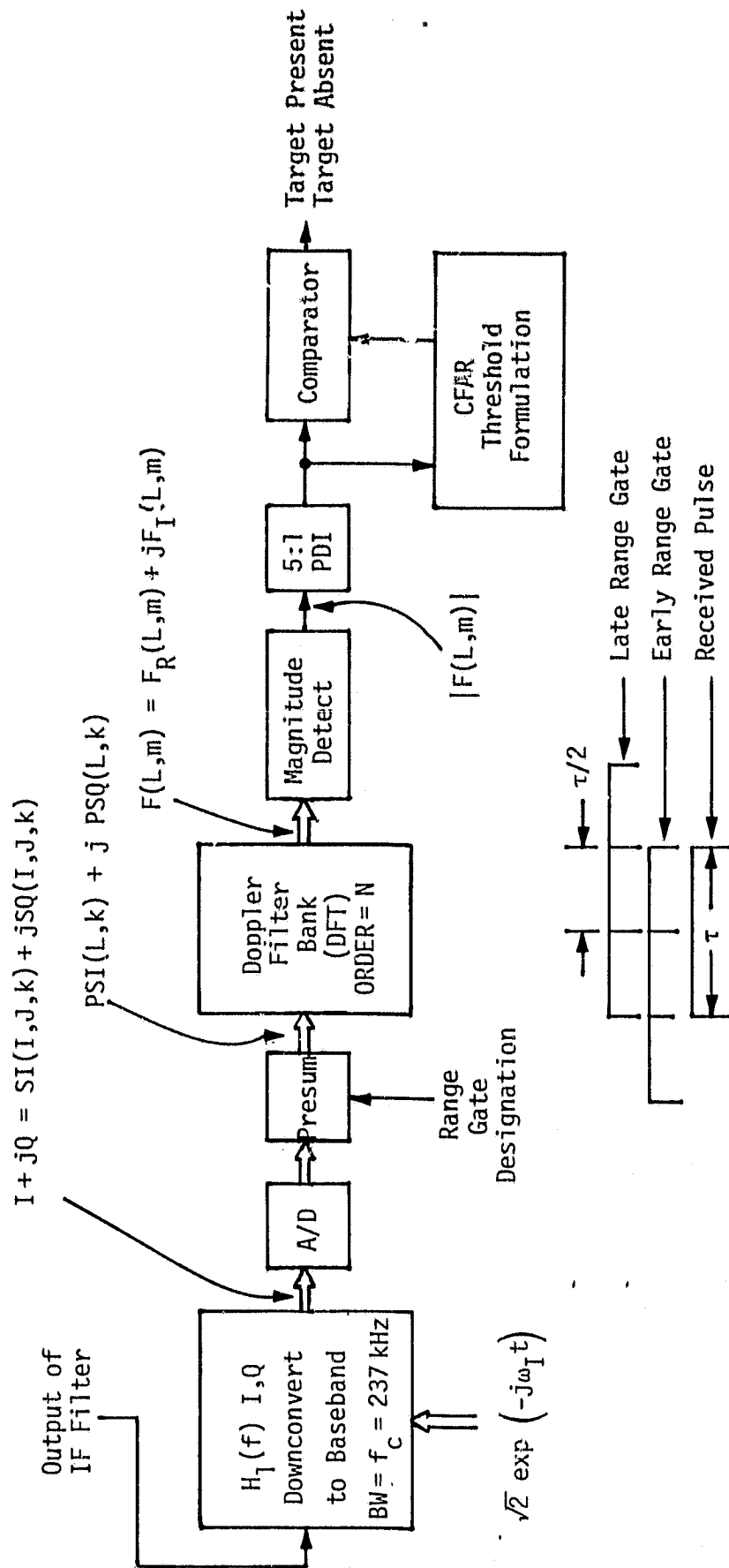
$$T_p = (\text{PRF})^{-1}$$

$N_c(t), N_s(t)$  = independent zero-mean Gaussian processes with one-sided power spectral density  $N_0$  W/Hz and one-sided noise bandwidth  $f_c$  ( $f_c = 237$  kHz), which is the 3 dB bandwidth of  $H_1(f)$  (see Figure 1).

The noise power in  $N_c(t)$  and  $N_s(t)$  is therefore given by

$$N_0 f_c \quad (3)$$

for each process.



Shuttle Ku-Band Radar

Figure 1. Signal Processing for Designated Mode in Search



The integration process of the presum is also shown in Figure 1 for the designated mode in search. We assume that the received pulse is ideally designated so that it appears exactly between the two range gates of width  $3\tau/2$ , as shown in Figure 1. This, coupled with neglecting the doppler effect, maximizes the effect of the signal received from the target on the CFAR threshold.

With these assumptions, the presum output for the  $k$ th pulse for the  $L$ th range gate is

$$\begin{aligned} \text{PSI}(L,k) + j \text{PSQ}(L,k) &= \frac{1}{\tau} \int_{t_s}^{t_s+3\tau/2} [\text{SI}(t) + j \text{SQ}(t)] dt \\ &= A_I \tau \exp(j\theta_I) + \int_{t_s}^{t_s+3\tau/2} [N_c(t) + j N_s(t)] dt \end{aligned} \quad (4)$$

where the sum of the samples at the output of the A/D is approximated by analog integration. This is an excellent approximation since the number of samples in  $3\tau/2$  is sufficiently large at long ranges. The starting time of the range gate integration is designated  $t_s$ .

The signal part of the presum output is designated

$$A_I \tau \exp(j\theta_I) = S_R(L,k) + j S_I(L,k) \quad (5)$$

where  $S_R$  and  $S_I$  are independent zero-mean Gaussian random variables, with variance  $\sigma_s^2$ . This is the same value found at the input to the presum because of the normalization in our definition.

The noise components of the presum output are designated

$$N_R(L,k) + j N_I(L,k) = \frac{1}{\tau} \int_{t_s}^{t_s+3\tau/2} [N_c(t) + j N_s(t)] dt \quad (6)$$

where  $N_R$  and  $N_I$  are independent Gaussian random variables with variances

$$\sigma_n^2 = \left(\frac{N_0}{2}\right) \frac{3}{2} = \frac{3}{4} N_0 \quad (7)$$

Formulation of the CFAR threshold for the designated mode in search is shown in more detail in Figure 2. In particular, the outputs of the DFT doppler filters are given by

$$F(m) = \sum_{k=0}^{N-1} \left[ \text{PSI}(k) + j \text{PSQ}(k) \right] \exp\left(-j \frac{2\pi mk}{N}\right) \quad (8)$$

for both the early and late range gate outputs. Note that the doppler filter outputs from the early and late range gates are correlated; this affects the evaluation of the variance of this CFAR threshold.

The CFAR threshold,  $T$ , is formed via the following average

$$T \triangleq C_1 \sum_{I=1}^{I_{\max}} \sum_{L=-1}^{+1} \sum_{m=0}^{N-1} F(L, m, I) \quad (9)$$

where

$I$  = the RF frequency index,  $I = 1, \dots, I_{\max}$ ,  $I_{\max} = 5$

$L$  = the range gate index,  $L=-1$ : early gate;  $L=+1$ : late gate

$k$  = the time or pulse index,  $k = 0, \dots, N-1$ ,  $N = 16$ .

$m$  = the frequency of doppler filter index,  $m = 0, \dots, N-1$ .

In the next section, the results of the statistical analysis of  $T$  are discussed.

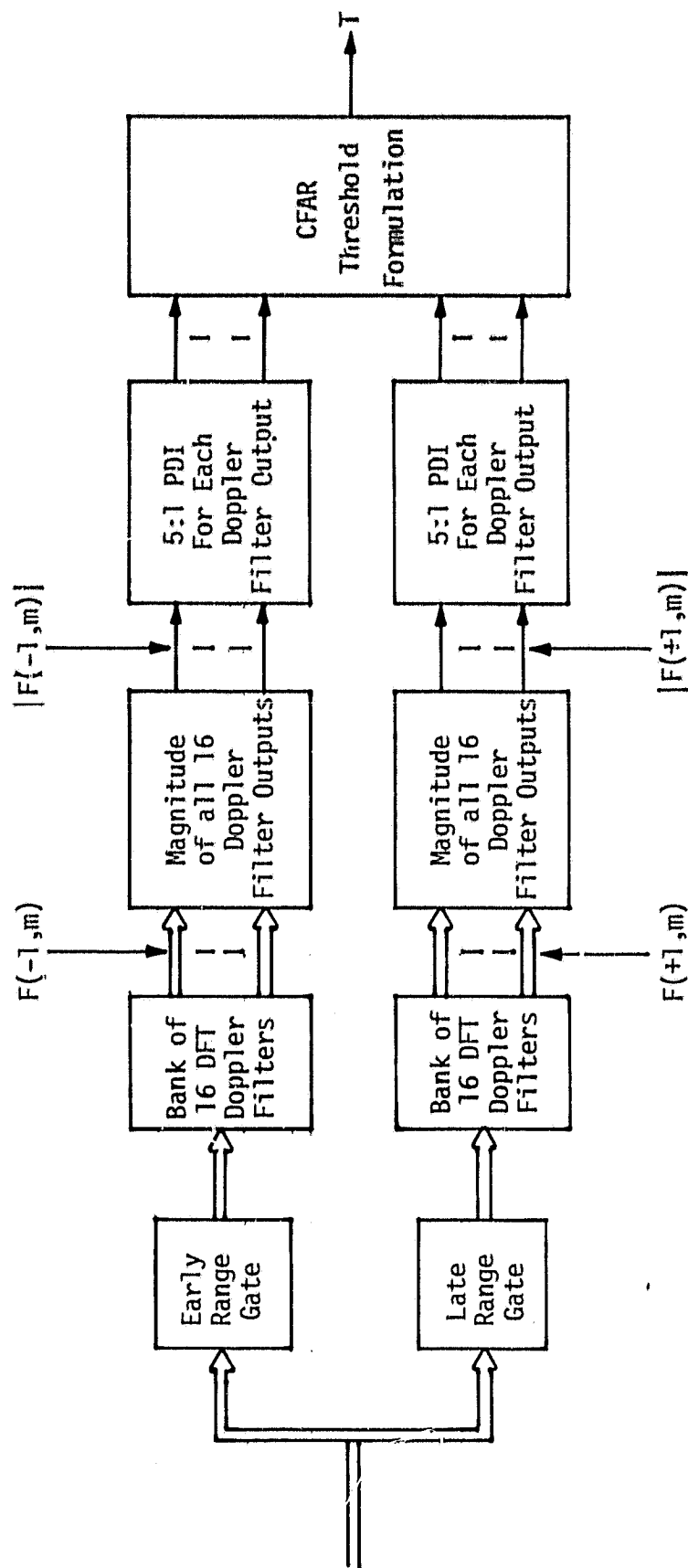


Figure 2. Formulation of Shuttle Ku-Band CFAR Threshold for Designated Mode in Search

### 3.0 PERFORMANCE OF CFAR THRESHOLD

The mean (ensemble average) of the CFAR threshold is determined in Appendix A and plotted in Figure 3. In this analysis, any doppler frequency shift away from the center frequency of the nearest doppler filter is neglected. In addition, it is assumed that the range designation is ideal. Both of these assumptions maximize the effect of the signal on the statistics of the CFAR threshold.

Under the above assumptions, the average CFAR threshold value for the designated mode versus the SNR at the output of the presum is plotted in Figure 3, where

$$\text{SNR} = \sigma_s^2 / \sigma_n^2 \quad (10)$$

As expected, at small values of SNR, the effect of the signal from the target disappears and the threshold becomes the value corresponding to noise only.

Also included in Figure 3 is the result of the simulation reported in [1]. The results of our analysis are normalized in Figure 3 so that the average threshold value at 0 dB coincides with that in [1].

At this time, we have no explanation for the significant difference between the exact analytical and the simulation results since their target dependence is less, even though we assumed maximum target dependence.

In Figure 4, the normalized standard deviation of the CFAR threshold is plotted versus the SNR at the output of the presum. This exact analytical result shows a significant dependence on SNR and a negligible dependence on the normalized noise correlation coefficient  $\rho$ . For the actual case, we have, as described for the range gates in Figure 1,

$$\rho = 2/3.$$

Inspection of the plot in Figure 4, however, shows little variation as  $\rho$  varies from 0 to 0.7

It is worthy to note the substantial variation in the CFAR threshold, particularly at large values of SNR where the normalized standard deviation is greater than 0.3. No attempt has been made to

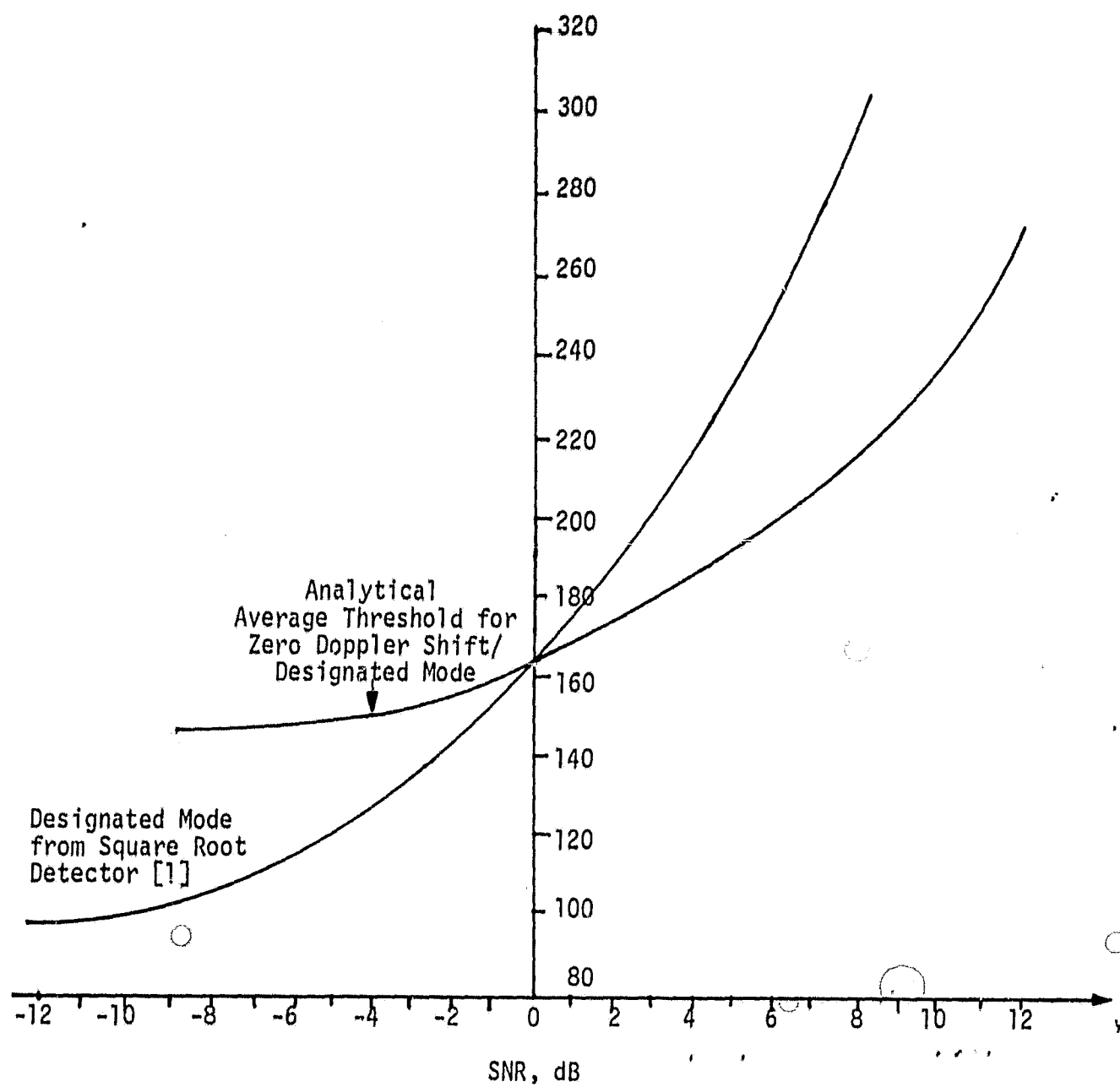


Figure 3. Average Threshold Values for Zero Doppler Shift, Designated Mode

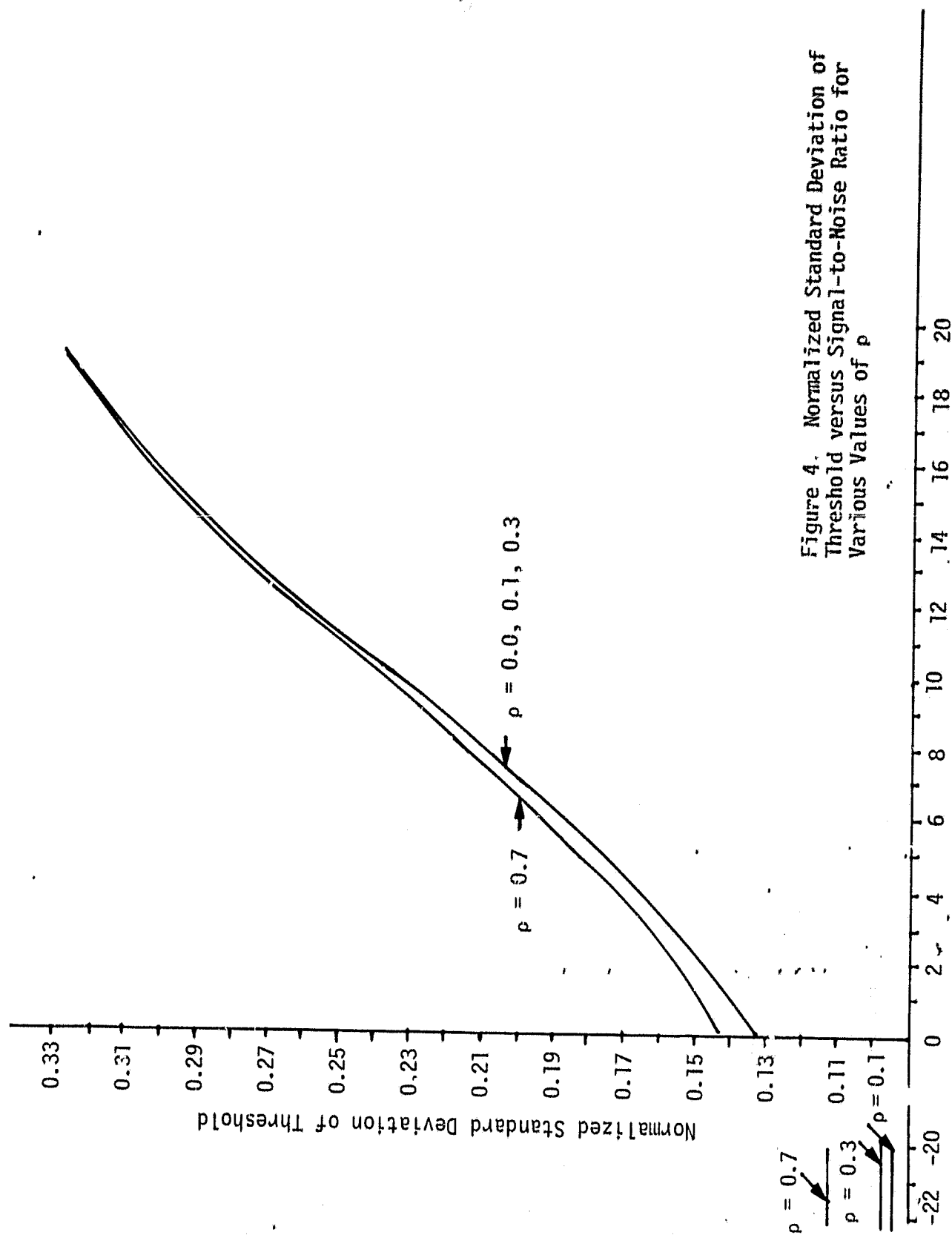


Figure 4. Normalized Standard Deviation of Threshold versus Signal-to-Noise Ratio for Various Values of  $\rho$

determine the effects of this variation on the probability of detection. On the optimistic side, the threshold setting and the target return are correlated; this leads us to conjecture that this variation may not appreciably affect the probability of detection. On the pessimistic side, there is a substantial variation of the CFAR threshold setting away from that developed from the noise-only condition.

## APPENDIX A

Here we wish to derive the expected value  $E\{T\}$  of the random variable  $T$ , defined as (see Figures 1 and 2):

$$T \triangleq C_1 \cdot \sum_{I=1}^{I_{\max}} \sum_{L=-1}^1 \sum_{m=0}^{N-1} |F(L, m, I)| \quad (1)$$

where the dependence of  $F$  on the frequency range  $I$  is explicitly shown in (1) and where  $C_1$  is a normalizing constant.

Before we proceed, let us first list the assumptions entailed in the following derivations.

### Assumptions

(1) The in-phase and quadrature-phase components of the signal and noise are zero-mean, independent, Gaussian random variables (rv).

(2) For different RF frequencies, all rv's are independent. We can therefore confine our interest to one specific frequency.

(3) For the same range gate ( $L$ ) and different time slots ( $k$ ), the noise variables are independent, i.e.,

$$\begin{aligned} N_R(L, k_1) &\perp N_R(L, k_2) && \text{for } k_1 \neq k_2 \\ N_I(L, k_1) &\perp N_I(L, k_2) \end{aligned}$$

(4) Real and imaginary parts of either signal or noise are always independent, i.e.,

$$N_R \perp N_I, \quad S_R \perp S_N, \quad \dots$$

(5) For the same  $k$  but different gate, the noise components are correlated. The covariance matrix is

$$R = \left\{ \text{cov} [N_R(-1, k), N_I(-1, k), N_R(1, k), N_I(1, k)] \right\} = \sigma_n^2 \begin{bmatrix} 1 & 0 & \rho & 0 \\ 0 & 1 & 0 & \rho \\ \rho & 0 & 1 & 0 \\ 0 & \rho & 0 & 1 \end{bmatrix}$$



Therefore, for different  $k$ 's, the noise rv's are independent, regardless of the value of  $L$ .

(6) For both range gates and all times  $k$  associated with one RF frequency, the parts of the signal are identical, i.e.,

$$S_R(-1, k_1) = S_R(-1, k_2) = S_R(1, k_3) = S_R(1, k_4),$$

for every  $k_1, k_2, k_3, k_4 \in [0, N]$ . Likewise for the imaginary parts of the signal  $S_I$ .

As an immediate result of assumption (2), the frequency dependence can be dropped and  $T$  can be written as

$$\begin{aligned} T &= C_1 \cdot I_{\max} \cdot \sum_{L=-1}^1 \sum_{m=0}^{N-1} |F(L, m)| \\ &= C \sum_{m=0}^{N-1} \sum_{L=-1}^1 |F(L, m)| \\ &= C \cdot \sum_{m=0}^{N-1} X(m) \end{aligned} \quad (2)$$

where  $C = C_1 \cdot I_{\max}$  and we have defined the rv  $X(m)$  by

$$X(m) = |F(-1, m)| + |F(1, m)| \quad (3)$$

In the following, we shall derive the expected value of  $X(m)$ . From (3), it follows that

$$E\{X(m)\} = E\{|F(-1, m)|\} + E\{|F(1, m)|\} \quad (4)$$

and, because of the symmetry existing between the two gates, (4) simplifies to

$$E\{X(m)\} = 2E\{|F(1, m)|\} \quad (5)$$

It is obvious from (5) and the assumptions made that the first moment

(ensemble average) is not a function of the range gate. Henceforth, we will drop the gate-index dependence from the symbols listed before in order to simplify matters.

Let us call

$$y(m) \triangleq |F(m)| = \sqrt{F_R^2(m) + F_I^2(m)} \quad (6)$$

so that, from (2), (5) and (6),

$$E\{T\} = 2C \cdot \sum_{m=0}^{N-1} E\{y(m)\} \quad (7)$$

Since  $F(m)$  is the output of a DFT filter whose input is the set  $\{\text{PSI}(k) + j\text{PSQ}(k)\}$ , we have that

$$F(m) = \sum_{k=0}^{N-1} (\text{PSI}(k) + j\text{PSQ}(k)) \cdot e^{-j \frac{2\pi mk}{N}}$$

which means that

$$F_R(m) = \sum_{k=0}^{N-1} \text{PSI}(k) \cos \frac{2\pi mk}{N} + \text{PSQ}(k) \sin \frac{2\pi mk}{N} \quad (8a)$$

$$F_I(m) = \sum_{k=0}^{N-1} -\text{PSI}(k) \sin \frac{2\pi mk}{N} + \text{PSQ}(k) \cos \frac{2\pi mk}{N} \quad (8b)$$

Since  $\text{PSI}(k)$ ,  $\text{PSQ}(k)$  are Gaussian rv's, (both signal and noise are Gaussian), so are their linear combinations  $F_R(m)$  and  $F_I(m)$ , which are also zero mean.

We will need the covariance matrix of  $\{F_R(m), F_I(m)\}$ . From (8a), we have that

$$\begin{aligned}
E\{F_R^2(m)\} = & E\left\{\sum_{k=0}^{N-1} \left(PSI(k) \cos \frac{2\pi mk}{N} + PSQ(k) \sin \frac{2\pi mk}{N}\right)^2\right. \\
& + \sum_{k=0}^{N-1} \sum_{\substack{\tau=0 \\ k \neq \tau}}^{N-1} \left(PSI(k) \cos \frac{2\pi mk}{N} + PSQ(k) \sin \frac{2\pi mk}{N}\right) \\
& \cdot \left(PSI(\tau) \cos \frac{2\pi m\tau}{N} + PSQ(\tau) \sin \frac{2\pi m\tau}{N}\right)\Bigg\} \quad (9)
\end{aligned}$$

But

$$E\{PSI^2(k)\} = E\{S_R^2(k) + N_R^2(k) + 2S_R(k) N_R(k)\} = \sigma_s^2 + \sigma_n^2 \quad (10a)$$

and, similarly,

$$E\{PSQ^2(k)\} = \sigma_s^2 + \sigma_n^2 \quad (10b)$$

For  $k \neq \tau$ ,

$$\begin{aligned}
E\{PSI(k) \cdot PSI(\tau)\} &= E\{(S_R(k) + N_R(k)) (S_R(\tau) + N_R(\tau))\} \quad (\text{Assumption 1}) \\
&= E\{S_R(k) \cdot S_R(\tau)\} + E\{N_R(k) N_R(\tau)\} \quad (\text{Assumptions 3,6}) \\
&= \sigma_s^2 \quad (11a)
\end{aligned}$$

and, similarly,

$$E\{PSQ(k) \cdot PSQ(\tau)\} = \sigma_s^2 \quad (11b)$$

Also, from Assumption 4,

$$E\{PSI(k) \cdot PSQ(k)\} = E\{PSI(k) \cdot PSQ(\tau)\} = E\{PSI(\tau) \cdot PSQ(k)\} = 0 \quad (12)$$

Substituting (10), (11), and (12) into (9) and after some manipulations, we get

$$E\{F_R^2(m)\} = (\sigma_s^2 + \sigma_n^2) \cdot \sum_{k=0}^{N-1} \left( \cos^2 \frac{2\pi mk}{N} + \sin^2 \frac{2\pi mk}{N} \right) \\ + \sigma_s^2 \sum_{k=0}^{N-1} \sum_{\substack{\tau=0 \\ k \neq \tau}}^{N-1} \left[ \cos \frac{2\pi m}{N} (k-\tau) \right]$$

or

$$E\{F_R^2(m)\} = N(\sigma_s^2 + \sigma_n^2) + 2\sigma_s^2 \sum_{\xi=1}^{N-1} (N-\xi) \cos \frac{2\pi m \xi}{N} \quad (13)$$

The corresponding result for  $E\{F_I^2(m)\}$  is easily shown to be the same as in (13).

Before we examine (13) closer, let us calculate the cross-covariance term:

$$E\{F_R(m) \cdot F_I(m)\} = E \left\{ \sum_{k=0}^{N-1} \sum_{\tau=0}^{N-1} \left( \text{PSI}(k) \cos \frac{2\pi mk}{N} + \text{PSQ}(k) \sin \frac{2\pi mk}{N} \right) \right. \\ \left. \times \left( -\text{PSI}(\tau) \sin \frac{2\pi m \tau}{N} + \text{PSQ}(\tau) \cos \frac{2\pi m \tau}{N} \right) \right\} \quad (\text{Assumption 4}) \\ = E \left\{ \sum_{k=0}^{N-1} \sum_{\tau=0}^{N-1} \left( -\text{PSI}(k) \text{PSI}(\tau) \sin \frac{2\pi m \tau}{N} \cos \frac{2\pi mk}{N} \right. \right. \\ \left. \left. + \text{PSQ}(k) \text{PSQ}(\tau) \cos \frac{2\pi m \tau}{N} \sin \frac{2\pi mk}{N} \right) \right\} \\ = \sigma_s^2 \sum_{k=0}^{N-1} \sum_{\substack{\tau=0 \\ k \neq \tau}}^{N-1} \sin \frac{2\pi m}{N} (k-\tau) \quad (14)$$

We now notice in (14) that, to each term  $\xi = k - \tau > 0$  in the double summation, there exists a corresponding term  $-\xi = \tau - k < 0$  which, because of the sine function being an odd function, cancels with the former term. Hence,

$$E\{F_R(m) \cdot F_I(m)\} = 0, \text{ for all } m \in [0, 15] \quad (15)$$

and this holds independently of  $N$ . The covariance matrix of  $F_R(m)$ ,  $F_I(m)$  can now be written as

$$\Lambda \triangleq \text{cov}\{F_R(m), F_I(m)\} = N \begin{bmatrix} A(m) \cdot \sigma_s^2 + \sigma_n^2 & 0 \\ 0 & A(m) \cdot \sigma_s^2 + \sigma_n^2 \end{bmatrix} \quad (16)$$

where, from (13) and (16), it follows that

$$A(m) = 1 + 2 \sum_{\xi=1}^{N-1} \left(1 - \frac{\xi}{N}\right) \cos \frac{2\pi m \xi}{N} \quad (17)$$

We will briefly examine  $A(m)$ . We have that, for  $m=0$ ,

$$\begin{aligned} A(0) &= 1 + 2 \sum_{\xi=1}^{N-1} \left(1 - \frac{\xi}{N}\right) = 1 + 2 \left[ (N-1) - \frac{1}{N} \sum_{\xi=1}^{N-1} \xi \right] \\ &= 1 + 2 \left[ N-1 - \frac{N(N-1)}{2N} \right] = N. \end{aligned} \quad (18)$$

To study the case  $m \neq 0$ , let us assume that  $N$  is divisible by 4. Then, if we call  $\xi' = N - \xi$ , it follows that

$$\cos \frac{2\pi m \xi'}{N} = \cos \frac{2\pi m}{N} (N - \xi) = \cos \frac{2\pi m \xi}{N}$$

so that (17) reduces to

$$A(m) = 1 + 2 \left[ \sum_{\xi=1}^{N/2-1} \left( 1 - \frac{\xi}{N} + 1 - \frac{N-\xi}{N} \right) \cos \frac{2\pi m \xi}{N} + \frac{\cos m \pi}{2} \right]$$

or

$$A(m) = 1 + 2 \sum_{\xi=1}^{N/2-1} \cos \frac{2\pi m \xi}{N} + \cos m \pi \quad (19)$$

If we now call  $\xi' = N/2 - \xi$ , it follows that

$$\cos \frac{2\pi m \xi'}{N} = \cos \frac{2\pi m (N/2 - \xi)}{N} = (-1)^m \cos \frac{2\pi m \xi}{N}$$

so that (19) yields

$$A(m) = 1 + 2 \left[ \sum_{\xi=1}^{N/4-1} \left( 1 + (-1)^m \right) \cos \frac{2\pi m \xi}{N} + \cos \frac{m \pi}{2} \right] + \cos m \pi \quad (20)$$

An immediate conclusion of (20) is that  $A(m) = 0$  for  $m = \text{odd}$ . For  $m = \text{even}$ , (20) reduces to

$$A(m) = 2 \left[ 1 + (-1)^{m/2} + 2 \sum_{\xi=1}^{N/4-1} \cos \frac{2\pi m \xi}{N} \right] \quad (21)$$

The above holds for an arbitrary  $N$  divisible by 4. In the general case, (21) might yield a nonzero value of  $A(m)$ , which nevertheless will be small. However, it is straightforward to show that, if  $N$  is a power of 2 (which is almost always the case in practice),  $A(m)$  of (21) identically vanishes. Below we summarize the conclusion for the covariance matrix  $\Lambda$ :

$$\Lambda = \text{cov}\{F_R(m), F_I(m)\} = \begin{cases} N \begin{bmatrix} N\sigma_s^2 + \sigma_n^2 & 0 \\ 0 & \sigma_s^2 + \sigma_n^2 \end{bmatrix} & ; m = 0 \\ N \begin{bmatrix} \sigma_n^2 & 0 \\ 0 & \sigma_n^2 \end{bmatrix} & ; m \neq 0 \end{cases} \quad (22)$$

From (22), some useful conclusions can be drawn. First, we notice that the noise components at the input affect all doppler filter outputs, while the effect of the signal is confined to the  $m=0$  doppler filter only. Furthermore, the effect of the signal on that term is enhanced by a factor of  $N$  as compared to the noise. Hence, for the moderate-to-high signal-to-noise ratio (SNR) environment, we can claim that the zeroth filter output is produced by the signal only and the other outputs by the noise only. Finally, we notice that, in all cases and for every doppler filter output, the real and imaginary parts of the output are independent. This enables us to conclude that  $y(m)$  of (6) is a Rayleigh rv with mean

$$E\{y(m)\} = \sqrt{\frac{\pi}{2}} \cdot \gamma(m) \quad (23)$$

where

$$\gamma(m) = \begin{cases} \sqrt{N^2\sigma_s^2 + N\sigma_n^2} & ; m = 0 \\ \sqrt{N\sigma_n^2} & ; m \neq 0 \end{cases} \quad (24)$$

From (7), (23) and (24), it follows that

$$E\{T\} = C\sqrt{2\pi} \cdot \left[ \sqrt{N^2\sigma_s^2 + N\sigma_n^2} + (N-1) \cdot \sqrt{N\sigma_n^2} \right]$$

or

$$E\{T\} = C \cdot N\sqrt{2\pi} \left[ \sqrt{\sigma_s^2 + \sigma_n^2/N} + \frac{N-1}{\sqrt{N}} \cdot \sigma_n \right] \quad (25)$$

or in terms of the signal-to-noise ratio  $SNR = \sigma_s^2 / \sigma_n^2$ ,

$$E\{T\} = C \cdot \sqrt{2\pi} \cdot N \cdot \sigma_n \left[ \sqrt{SNR + \frac{1}{N}} + \frac{N-1}{\sqrt{N}} \right] \quad (26)$$

Typically, the constant  $C_1$  in (1) is defined as

$$C_1 = \frac{1}{2NI_{\max}} \quad (27)$$

In this case,  $C = C_1 \cdot I_{\max} = 1/2N$ , and (26) modifies to

$$E\{T\} = \sqrt{\frac{\pi}{2}} \cdot \sigma_n \cdot \left[ \sqrt{SNR + \frac{1}{N}} + \frac{N-1}{\sqrt{N}} \right] \quad (28)$$

For the specific application considered,  $N = 16$ , so that the factor  $1/N \approx 0.06$  can be neglected for even very moderate SNR (say,  $SNR \geq 0$  dB). In this case, we conclude that  $E\{T\}$  varies linearly with  $(SNR)^{1/2}$ .

A final comment pertains to the values of SNR and  $\sigma_n^2$  of (28). These are the values of the signal-to-noise ratio and noise power at the input of the doppler filters. Since an A/D converter precedes these filters, the values of these parameters at the input of the A/D converter, denoted here by  $(SNR)_i$  and  $\sigma_{n_i}$ , respectively, relate to the A/D output parameters (which are the inputs to the filters) by [2]:

$$SNR = \frac{SNR_i}{L_{A/D}} \quad (29a)$$

and

$$\sigma_n = \sigma_{n_i} \sqrt{L_{A/D}} \quad (29b)$$

where

$$L_{A/D} = 1.0129 + 0.0129 \cdot SNR_i \quad (30)$$



If we incorporate (29) and (30) into (28), we get

$$E\{T\} = \sqrt{\frac{\pi}{2}} \cdot \sigma_{n_i} \cdot \sqrt{L_{A/D}} \left[ \sqrt{\frac{SNR_i}{L_{A/D}}} + \frac{N-1}{\sqrt{N}} \right] \quad (31)$$

which is plotted in Figure 3 for  $N = 16$  as a function of  $SNR_i$  in dB.

## APPENDIX B

We evaluate herein the variance  $\sigma_T^2$  of the random variable  $T$ , as defined in equation (1) of Appendix A.

From (2) of Appendix A, it follows that:

$$E\{T^2\} = c^2 \cdot \left[ \sum_{m=0}^{N-1} x^2(m) + \sum_{\substack{m_1=0 \\ m_1 \neq m_2}}^{N-1} \sum_{m_2=0}^{N-1} x(m_1) x(m_2) \right] \quad (1)$$

where

$$x(m) = \sqrt{F_R^2(-1,m) + F_I^2(-1,m)} + \sqrt{F_R^2(1,m) + F_I^2(1,m)} \quad (2)$$

To simplify matters, we will examine two distinct cases: moderate-to-high and low SNR.

### 1.0 MODERATE-TO-HIGH SNR

According to the previous comments of Appendix A, we can justifiably assume in this case that the zeroth doppler filter output  $x(0)$  is produced by the signal part of the DFT input only, while all other  $x(m)$ ,  $m \neq 0$  are produced by noise only.

#### 1.1 Signal Output ( $m=0$ )

$$E\{x^2(0)\} = (\text{from (2)}) = E\left\{F_R^2(-1,0) + F_I^2(-1,0) + F_R^2(1,0) + F_I^2(1,0) + 2\sqrt{(F_R^2(-1,0) + F_I^2(-1,0))(F_R^2(1,0) + F_I^2(1,0))}\right\} \quad (3)$$

Since we have assumed that all random variables appearing in (3) are exclusively signal functions, we can further invoke Assumption 6 of Appendix A, according to which

$$F_R(-1,0) = F_R(1,0) \quad \text{and} \quad F_I(-1,0) = F_I(1,0).$$

Substituting the above into (3) yields

$$E\{X^2(0)\} = 4E\{F_R^2(-1,0)\} + 4E\{F_I^2(-1,0)\} \quad (4)$$

From (22) of Appendix A, we have (setting  $\sigma_s^2 \gg \sigma_n^2$ ) that

$$E\{F_R^2(-1,0)\} = E\{F_I^2(-1,0)\} = N^2 \sigma_s^2 \quad (5)$$

so that (4) and (5) combine to give

$$E\{X^2(0)\} = 8N^2 \sigma_s^2 \quad (6)$$

## 1.2 Noise Outputs ( $m \neq 0$ )

$$E\{X^2(m)\}_{m \neq 0} = E\{F_R^2(-1,m) + F_I^2(-1,m) + F_R^2(1,m) + F_I^2(1,m) + 2\sqrt{(F_R^2(-1,m) + F_I^2(-1,m))(F_R^2(1,m) + F_I^2(1,m))}\} \quad (7)$$

Since all random variables are produced by noise, it follows from (22) of Appendix A that

$$E\{F_R^2(-1,m)\} = E\{F_I^2(1,m)\} = E\{F_R^2(1,m)\} = E\{F_I^2(-1,m)\} = N\sigma_n^2 \triangleq \sigma^2$$

so that

$$E\{X^2(m)\}_{m \neq 0} = 4N\sigma_n^2 + 2D \quad (8)$$

where

$$D \triangleq E\left\{\sqrt{(F_R^2(-1,m) + F_I^2(-1,m))(F_R^2(1,m) + F_I^2(1,m))}\right\} \quad (9)$$

We now proceed to evaluate  $D$ . To do this, we need the joint statistics of the zero-mean, Gaussian rv's appearing in (9). Let us find the covariance matrix  $R$  of  $\{F_R(-1,m), F_I(-1,m), F_R(1,m), F_I(1,m)\}$ ,  $m \neq 0$ .

From (8a) of Appendix A, we have that (assuming only noise input),

$$E\{F_R^2(-1, m)\} = E\left\{\left[\sum_{k=0}^{N-1} \left(N_R(k, -1) \cos \frac{2\pi mk}{N} + N_I(k, -1) \sin \frac{2\pi mk}{N}\right)\right]^2\right\}$$

(because of assumption 4)

$$= \sigma_n^2 \sum_{k=0}^{N-1} \left(\cos^2 \frac{2\pi mk}{N} + \sin^2 \frac{2\pi mk}{N}\right) = N\sigma_n^2 = \sigma^2 \quad (10)$$

and similarly for the others.

Furthermore,

$$E\{F_R(-1, m) \cdot F_R(1, m)\} = E\left\{\sum_{k=0}^{N-1} \sum_{\tau=0}^{N-1} \left(N_R(-1, k) \cos \frac{2\pi mk}{N} + N_I(-1, k) \sin \frac{2\pi mk}{N}\right) \right. \\ \left. \left(N_R(1, \tau) \cos \frac{2\pi m\tau}{N} + N_I(1, \tau) \sin \frac{2\pi m\tau}{N}\right)\right\} \quad (11)$$

which, because of Assumptions 4 and 5, reduces to

$$E\{F_R(-1, m) \cdot F_R(1, m)\} = E\left\{\sum_{k=0}^{N-1} N_R(-1, k) N_R(1, k) \cos^2 \frac{2\pi mk}{N} \right. \\ \left. + N_I(-1, k) \cdot N_I(1, k) \sin^2 \frac{2\pi mk}{N}\right\} = N \cdot \sigma_n^2 \cdot \rho = \rho \sigma^2 \quad (12)$$

Hence, the covariance matrix  $R$  is

$$R = \text{cov}\{F_R(-1, m), F_I(-1, m), F_R(1, m), F_I(1, m)\} = \sigma^2 \begin{bmatrix} 1 & 0 & \rho & 0 \\ 0 & 1 & 0 & \rho \\ \rho & 0 & 1 & 0 \\ 0 & \rho & 0 & 1 \end{bmatrix} \quad (13)$$

Comparing (13) and Assumption 5, we draw the interesting conclusion that the noise statistics remain unaltered after passing through the complex DFT doppler filters.

We are now in a position to evaluate D. If we change to polar coordinates

$$\begin{aligned} F_R(-1, m) &= V_E \cos \phi_E & F_R(1, m) &= V_L \cos \phi_L \\ &\text{and} & & \\ R_I(-1, m) &= V_E \sin \phi_E & F_I(1, m) &= V_L \sin \phi_L \end{aligned} \quad (14)$$

then (9) is simply written as

$$D = E\{V_E \cdot V_L\} \quad (15)$$

The joint distribution of the envelopes  $V_E$  and  $V_L$ , for the four Gaussian rv's correlated as in (13), is found from [3] to be

$$\rho(V_E, V_L) = \begin{cases} \frac{V_E V_L}{|R|^{1/2}} \cdot I_0 \left( \frac{V_E V_L \sigma^2 \rho}{|R|^{1/2}} \right) \cdot \exp \left\{ - \frac{\sigma^2 (V_E^2 + V_L^2)}{2|R|^{1/2}} \right\} & , \text{ for } V_E, V_L \geq 0 \\ 0 & , \text{ elsewhere} \end{cases} \quad (16)$$

where  $I_0(\cdot)$  is the zeroth-order modified Bessel function. From (15) and (16), it follows that

$$D = \int_0^\infty \int_0^\infty \frac{V_E^2 V_L^2}{|R|^{1/2}} \cdot I_0 \left( \frac{V_E V_L \sigma^2 \rho}{|R|^{1/2}} \right) \cdot \exp \left\{ - \frac{\sigma^2 (V_E^2 + V_L^2)}{2|R|^{1/2}} \right\} dV_E dV_L \quad (17)$$

If we make the transformation

$$V_E^2 = \frac{|R|^{1/2}}{\sigma^2} \cdot y \cdot \exp \{2z\}$$

$$V_L^2 = \frac{|R|^{1/2}}{\sigma^2} \cdot y \exp \{-2z\}$$

whose Jacobian is

$$|J| = \frac{|R|^{1/2}}{\sigma^2}$$

and, upon substituting into (17), we get

$$D = \frac{|R|}{\sigma^6} \int_0^\infty dy \cdot y^2 \cdot I_0(j\rho y) \cdot \left( \int_{-\infty}^\infty dz \cdot \exp\{-y \cosh(2z)\} \right) \quad (18)$$

The inner integral equals  $K_0(y)$  [4], where  $K_0(y)$  is the zeroth-order modified Hankel function. Therefore, from (18),

$$D = \frac{|R|}{\sigma^6} \int_0^\infty y^2 J_0(j\rho y) K_0(y) dy \quad (19)$$

where we have used the fact that  $I_0(n) = J_0(jn)$  ( $J_0(\cdot)$  is the zeroth-order Bessel function).

The integral of (19) can be evaluated. From [5], we find that

$$\begin{aligned} \int_0^\infty K_\alpha(az) J_\beta(bz) \cdot z^{-\gamma} dz \\ = b^\beta \cdot \Gamma\left(\frac{\beta-\gamma+\alpha+1}{2}\right) \cdot \Gamma\left(\frac{\beta-\gamma-\alpha+1}{2}\right) \cdot 2^{-(\gamma+1)} \cdot a^{\gamma-\beta-1} \Gamma^{-1}(\beta+1) \\ \cdot {}_2F_1\left(\frac{\beta-\gamma+\alpha+1}{2}; \frac{\beta-\gamma-\alpha+1}{2}; \beta+1; -\frac{b^2}{a^2}\right) \end{aligned} \quad (20)$$

where  ${}_2F_1(\cdot)$  is the Gaussian hypergeometric function [5]. Applying (20) for  $\alpha=0$ ,  $\beta=0$ ,  $\gamma=-2$ ,  $a=1$ ,  $b=j\rho$ , we get from (19) that

$$D = \frac{|R|}{\sigma^6} \cdot \frac{\pi}{2} \cdot {}_2F_1(3/2; 3/2; 1; \rho^2) \quad (21)$$

From [5], we find that

$$\begin{aligned} {}_2F_1(3/2; 3/2; 1; \rho^2) &= (1-\rho^2)^{-2} \cdot {}_2F_1(-1/2; -1/2; 1; \rho^2) \\ &= (1-\rho^2)^{-2} \cdot \left[ \frac{4}{\pi} E(\rho^2) - \frac{2}{\pi} (1-\rho^2) \cdot k(\rho^2) \right] \end{aligned} \quad (22)$$

where  $k(\cdot)$  and  $E(\cdot)$  are the complete elliptic integrals of the first and second kind [6].

Upon substitution of (22) into (21), we find that

$$D = \frac{|R|}{\sigma^6} \cdot (1-\rho^2)^{-2} \left[ 2E(\rho^2) - (1-\rho^2) k(\rho^2) \right] \quad (23)$$

From (13), the determinant  $|R|$  can be evaluated to be

$$|R| = \sigma^8 (1-\rho^2) = N^4 \sigma_n^8 (1-\rho^2)^2 \quad (24)$$

From (23) and (24), we finally get

$$D = N \sigma_n^2 \left[ 2E(\rho^2) - (1-\rho^2) k(\rho^2) \right] \quad (25)$$

From (8) and (25), we derive that

$$E \left\{ X(m)^2 \right\}_{m \neq 0} = 2N \sigma_n^2 \left[ 2 + 2E(\rho^2) - (1-\rho^2) k(\rho^2) \right] \quad (26)$$

Equations (6) and (26) yield the result for the first summation in (1). The second term (double summation) is now evaluated.

First let us assume that  $m_1 \neq m_2$  and none of them equals zero. In this case, both  $X(m_1)$  and  $X(m_2)$  are produced by noise, and from (2),

$$\begin{aligned}
E \left\{ X(m_1) X(m_2) \right\}_{0 \neq m_1 \neq m_2 \neq 0} &= E \left\{ \sqrt{(F_R^2(-1, m_1) + F_I^2(-1, m_1)) \cdot (F_R^2(-1, m_2) + F_I^2(-1, m_2))} \right\} \\
&+ E \left\{ \sqrt{(F_R^2(1, m_1) + F_I^2(1, m_1)) \cdot (F_R^2(1, m_2) + F_I^2(1, m_2))} \right\} \\
&+ E \left\{ \sqrt{(F_R^2(-1, m_1) + F_I^2(-1, m_1)) \cdot (F_R^2(1, m_2) + F_I^2(1, m_2))} \right\} \\
&+ E \left\{ \sqrt{(F_R^2(1, m_1) + F_I^2(1, m_1)) \cdot (F_R^2(-1, m_2) + F_I^2(-1, m_2))} \right\} \quad (27)
\end{aligned}$$

We will now show that all random variables under the same square root are mutually independent. To do this, let us evaluate

$$\begin{aligned}
E \left\{ F_R(-1, m_1) \cdot F_R(-1, m_2) \right\}_{m_1 \neq m_2} &= E \left\{ \sum_{k=0}^{N-1} \sum_{\tau=0}^{N-1} \left( N_R(-1, k) \cos \frac{2\pi m_1 k}{N} + N_I(-1, k) \sin \frac{2\pi m_1 k}{N} \right) \right. \\
&\quad \cdot \left. \left( N_R(-1, \tau) \cos \frac{2\pi m_2 \tau}{N} + N_I(-1, \tau) \sin \frac{2\pi m_2 \tau}{N} \right) \right\} \\
&\quad \text{(Assumption 4)} \\
&= E \left\{ \sum_{k=0}^{N-1} N_R^2(-1, k) \cos \frac{2\pi m_1 k}{N} \cos \frac{2\pi m_2 k}{N} \right. \\
&\quad \left. + N_I^2(-1, k) \sin \frac{2\pi m_1 k}{N} \sin \frac{2\pi m_2 k}{N} \right\} \\
&= \sigma_n^2 \sum_{k=0}^{N-1} \cos \frac{2\pi k(m_1 - m_2)}{N} \quad (28)
\end{aligned}$$

For  $N$  a power of 2 and  $m_1 \neq m_2$ , it is easy to show that the summation in (28) vanishes which, in turn, means that  $F_R(-1, m_1)$  and  $F_R(-1, m_2)$  are independent. Identically, we show that  $F_I(-1, m_1) \perp F_I(-1, m_2)$ . Similarly,



$$E\{F_R(-1, m_1) \cdot F_R(1, m_2)\} = \rho \sigma_n^2 \sum_{k=0}^{N-1} \cos \frac{2\pi k(m_1 - m_2)}{N} = 0.$$

Finally, by interchanging 1 and -1, we get the symmetrical results for both gates, which justify our earlier claim that all rv's in (27) are independent. Therefore,

$$\begin{aligned} E\left\{X(m_1) X(m_2)\right\}_{\substack{0 \neq m_1 \neq m_2 \neq 0}} &= 4E^2\left\{\sqrt{F_R^2(-1, m_1) + F_I^2(-1, m_1)}\right\} \\ &= 4 \cdot \left(\sigma \sqrt{\frac{\pi}{2}}\right)^2 = 2\pi N \sigma_n^2 \end{aligned} \quad (29)$$

Second, assume that  $m_1 = m_2 = m \neq 0$ . Because  $X(0)$  is produced by the signal,  $X(m)$  by the noise and, due to the high SNR assumption, we get

$$\begin{aligned} E\{X(m) X(0)\}_{m \neq 0} &= E\{X(m)\} \cdot E\{X(0)\} \quad (\text{see (22) of Appendix A}) \\ &= \sqrt{2\pi} \cdot \sqrt{N^2 \sigma_s^2} \cdot \sqrt{2\pi} \cdot \sqrt{N \sigma_n^2} = 2 N \sqrt{N} \sigma_s \sigma_n \end{aligned} \quad (30)$$

From the  $N^2$  terms involved in (1), one term is given by (6),  $(N-1)$  terms are given by (26),  $2(N-1)$  terms are given by (30) and  $(N-1) \cdot (N-2)$  terms are given by (29). Summarizing, we get that

$$\begin{aligned} E\{T^2\} &= C^2 \cdot \left[ 8N^2 \sigma_s^2 + (N-1) \cdot 2N \sigma_n^2 \left[ 2 + 2E(\rho^2) - (1-\rho^2) K(\rho^2) \right] \right. \\ &\quad \left. + 2(N-1) \cdot 2\pi N \sqrt{N} \sigma_s \sigma_n + (N-1)(N-2) 2\pi N \sigma_n^2 \right] \\ &= 2C^2 N^2 \sigma_n^2 \left[ 4 \cdot \text{SNR} + \left(1 - \frac{1}{N}\right) \left[ 2 + 2E(\rho^2) - (1-\rho^2) K(\rho^2) \right] \right. \\ &\quad \left. + \frac{2\pi(N-1)}{\sqrt{N}} \sqrt{\text{SNR}} + \left(1 - \frac{1}{N}\right) \cdot (N-2) \cdot \pi \right] \end{aligned} \quad (31)$$

But from (28) of Appendix A, we have that (for high SNR)

$$E\{T\} = C \cdot N\sqrt{2\pi} \cdot \sigma_n \left[ \sqrt{\text{SNR}} + \left( \frac{N-1}{\sqrt{N}} \right) \right]$$

therefore,

$$E^2\{T\} = 2C^2N^2 \cdot \sigma_n^2 \cdot \left[ \pi \text{SNR} + \frac{\pi(N-1)^2}{N} + \frac{2\pi(N-1) \cdot \sqrt{\text{SNR}}}{\sqrt{N}} \right] \quad (32)$$

From (31) and (32), it follows that

$$\begin{aligned} \text{var}\{T\} &= \sigma_T^2 \\ &= E\{T^2\} - E^2\{T\} \\ &= 2C^2N^2\sigma_n^2 \left[ (4-\pi) \text{SNR} + \left( 1 - \frac{1}{N} \right) \left[ 2 + 2E(\rho^2) - (1-\rho^2) K(\rho^2) \right. \right. \\ &\quad \left. \left. + (N-2)\pi - (N-1)\pi \right] \right] \end{aligned}$$

or

$$\sigma_T^2 = 2C^2N^2\sigma_n^2 \left[ (4-\pi) \text{SNR} + \left( 1 - \frac{1}{N} \right) H(\rho) \right]$$

where

$$H(\rho) = 2 - \pi + 2E(\rho^2) - (1-\rho^2) K(\rho^2)$$

(33)

(Moderate-to-high SNR)

The primary quantity of interest is the ratio  $\sigma_T/E\{T\}$  which, for case 1.1 is given by

$$\frac{\sigma_T}{E\{T\}} = \frac{\sqrt{2}C N \sigma_n \sqrt{(4-\pi) \text{SNR} + \left( 1 - \frac{1}{N} \right) H(\rho)}}{C N_0 \sqrt{2\pi} \cdot G_n \left( \sqrt{\text{SNR}} + \frac{N-1}{\sqrt{N}} \right)}$$

or

$$\frac{\sigma_T}{E\{T\}} = \frac{1}{\sqrt{\pi}} \cdot \frac{\sqrt{(4-\pi) \text{SNR} + \left(1 - \frac{1}{N}\right) H(\rho)}}{\left(\sqrt{\text{SNR}} + \frac{N-1}{\sqrt{N}}\right)} \quad (34)$$

(Moderate-to-high SNR)

## 2.0 VERY LOW SNR (OR SIGNAL ABSENT)

In this case, all the doppler filter outputs are produced by noise. If signal is also present (in order for this assumption to be valid, even for the  $m=0$  filter), we must have that

$$N\sigma_s^2 \ll \sigma_n^2 \rightarrow \frac{\sigma_s^2}{\sigma_n^2} \ll \frac{1}{N}.$$

For  $N=16$ , such an inequality is satisfied for SNR in the order of -20 dB or less.

From (26) (which also holds for  $m=0$  now) and (29) (which is now restricted only to  $m_1 \neq m_2$ ), we get that

$$\begin{aligned} E\{T^2\} &= C^2 \left[ 2N^2\sigma_n^2 \left[ 2 + 2E(\rho^2) - (1-\rho^2) k(\rho^2) \right] + N(N-1) 2\pi N\sigma_n^2 \right] \\ &= 2C^2 N^2\sigma_n^2 \left[ 2 + (N-1) + 2E(\rho^2) - (1-\rho^2) k(\rho^2) \right] \end{aligned} \quad (35)$$

For very low SNR, we have from (28) of Appendix A that

$$E\{T\} = C \cdot \sqrt{2\pi} \cdot N \cdot \sqrt{N\sigma_n^2}$$

therefore

$$E^2\{T\} = 2\pi C^2 N^3 \sigma_n^2$$

and

$$\text{var}\{T\} = \sigma_T^2 = 2C^2N^2\sigma_n^2 \left[ 2 + (N-1)\pi + 2E(\rho^2) - (1-\rho^2) K(\rho^2) - N\pi \right]$$

or

$$\text{var}\{T\} = 2C^2N^2\sigma_n^2 \cdot H(\rho) \quad (36)$$

where  $H(\rho)$  has been defined in (33). The ratio  $\sigma_T/E\{T\}$  for this case (2.0) is found to be

$$\frac{\sigma_T}{E\{T\}} = \frac{\sqrt{2}NC\sigma_n\sqrt{H(\rho)}}{\sqrt{2} \cdot C \cdot N\sqrt{N} \cdot \sigma_n}$$

or

$$\boxed{\frac{\sigma_T}{E\{T\}} = \sqrt{\frac{H(\rho)}{N\pi}}} \quad (37)$$

(Very low SNR)

independent of the SNR, as expected. The ratios of (36) and (37) have been plotted in Figure 4 for various values of  $\rho$ . The function  $H(\rho)$  depends on the complete elliptic integrals  $E(\rho^2)$  and  $K(\rho^2)$ , which have been tabulated for different values of the argument  $\rho^2$  [6]. In Table 1, we give some values of  $H(\rho)$  as a function of  $\rho$ .

Table 1.

$\rho$	0.0	0.1	0.2	0.3	0.4	0.5	0.6	0.7	0.8	0.9	0.99
$H(\rho^2)$	0.42920	0.43313	0.44495	0.46475	0.49269	0.52902	0.57409	0.72843	0.69280	0.76850	0.84851

## REFERENCES

1. Shingledecker, D.K., and Magnusson, H.G., "Results of Computer Analysis of Ku-Band Radar Search Mode Detection Probability," Hughes Aircraft Company, IDC #2705.00/109.
2. Weber, C.L., and Alem, W.K., "Study to Investigate and Evaluate Means of Optimizing the Ku-Band Combined Radar/Communication Functions for the Space Shuttle," Axiomatix Report No. R7710-5, October 28, 1977.
3. Davenport, W.B., Jr., and Root, W.L., Random Signals and Noise, McGraw-Hill, 1958, Chapter 8, page 163.
4. Magnus, W., and Oberhettinger, F., Special Functions of Mathematical Physics, Chelsea, NY, 1949, Chapter III.
5. Middleton, D., Introduction to Statistical Communication Theory, McGraw-Hill, 1960, Appendix C.
6. "Handbook of Mathematical Functions with Formulas, Graphs and Mathematical Tables," U.S. Dept. of Commerce, National Bureau of Standards, Chapter 17.